arXiv:cond-mat/0610276v1 [cond-mat.str-el] 10 Oct 2006

Dirty Peierls transition to stripe phase in manganites

S. Cox,[1,2] J.C. Lashley,[3] E. Rosten,[3] J. Singleton,[1] A.J. Williams,[4] and P.B. Littlewood[5]

[1] *National High Magnetic Field Laboratory, Los Alamos National Laboratory, Ms-E536, Los Alamos, New Mexico, 87545, USA*
[2] *Department of Materials Science and Metallurgy, University of Cambridge, Cambridge, CB2 3QZ, UK*
[3] *Los Alamos National Laboratory, Los Alamos, New Mexico, 87545, USA*
[4] *Centre for Science at Extreme Conditions, University of Edinburgh, Edinburgh, EH9 3JZ, UK*
[5] *Cavendish Laboratory, University of Cambridge, Cambridge, CB3 0HE, UK*

The nature of the phase transitions in $La_{1-x}Ca_xMnO_3$ and $Pr_{0.48}Ca_{0.52}MnO_3$ has been probed using heat capacity and magnetisation measurements. The phase transition associated with the onset of the stripe phase has been identified as second order. The model of a Peierls transition in a disordered system (a 'dirty' Peierls transition) is shown to provide an extremely good fit to this transition. In addition, an unexpected magnetic phase has been revealed in low temperature $Pr_{0.48}Ca_{0.52}MnO_3$, associated with an excess heat capacity over a wide temperature range compared to $La_{0.48}Ca_{0.52}MnO_3$.

PACS numbers: 75.47.Lx, 71.45.Lr, 65.40.Ba, 65.40.Gr

Many strongly correlated electron systems (e.g. manganites [1, 2], cuprates [3], nickelates [4] and cobaltites [5]) exhibit charge ordering phenomena, in which a superstructure forms at low temperatures. The insulating nature of the compounds and the results of transmission electron microscopy (TEM) experiments [1, 2, 6] led to the suggestion that the superstructure formation was driven by charge separation and localisation at atomic sites. However, recent work has produced conflicting evidence as to the nature of the superstructure, with some studies supporting a model with charge localised at the atomic sites, but with the difference in charge between atomic sites being small [7, 8, 9, 10, 11], and others indicating the the superstructure is not tied to the atomic sites [12, 13]. To explain the latter results, it has been proposed that the superstructure resembles a charge density wave (CDW) [12, 14]. In this paper, we find strong support for a CDW model of the superstructure in manganites.

Previous measurements of $La_{1-x}Ca_xMnO_3$ with $x \geq 0.5$ [15, 16, 17, 18] have observed two transitions as peaks in the heat capacity. The peak at higher temperature (T) was attributed to critical fluctuations of the order-disorder type associated with charge ordering [16, 18], with a contribution at $x = 0.5$ from the onset of ferromagnetism (FM). The transition was identified as first order based on the hysteresis in the resistivity data [17]. The lower T peak was attributed to the transition from a paramagnetic state to an antiferromagnetic (AFM) state [15, 16, 17, 18].

Here we use heat capacity and magnetisation measurements to gain insight into the nature of the phase transitions in manganites. $La_{0.50}Ca_{0.50}MnO_3$, $La_{0.48}Ca_{0.52}MnO_3$ and $Pr_{0.48}Ca_{0.52}MnO_3$ were measured, with the latter two being chosen as compounds with different average cation sizes and variances (see Table I) but in which the superstructure has on average an almost identical wavevector [13]. The smaller size of the Pr cation is thought to lead to stronger electron-phonon coupling, allowing the superstructure to lock into the lattice in around 25% of the grains [13]. The $La_{0.50}Ca_{0.50}MnO_3$ sample was chosen as it has a nominally commensurate superstructure (though small deviations are seen in TEM measurements [19]) and so provides a contrast between commensurate and incommensurate systems.

	Average Re/Ae site radius (Å)	Variance of Re/Ae site radius (Å^2)
$La_{0.50}Ca_{0.50}MnO_3$	1.198	3.24×10^{-4}
$La_{0.48}Ca_{0.52}MnO_3$	1.197	3.23×10^{-4}
$Pr_{0.48}Ca_{0.52}MnO_3$	1.180	2.50×10^{-7}

TABLE I: Average and variance of the radius of the site occupied by rare earth (Re) or alkaline earth (Ae) ions in different compositions of $Re_{1-x}Ae_xMnO3$ (the Re/Ae site radius). Here Re is La or Pr, Ae is Ca and x=0.5 or 0.52. [20].

Samples were prepared by repeated grinding, pressing and sintering of appropriate oxides and carbonates in stoichiometric proportions. The carbonates were decarboxylated by heating for 12 hours at 950°C. Each sample was reground, repelleted and heated at 1350°C for 4 days, then reground, repelleted and reheated at 1350°C for another 4 days. X-ray powder diffraction indicated that the samples were single phase [21].

Heat capacity measurements were made using a Quantum Design Physical Properties Measurement System (PPMS). The accuracy of the measurements can be checked by examining the fits to the PPMS-measured decay curves. This is especially important in the region of a first order transition, where the release of latent heat can reduce the quality of the fit [22]. In order to ensure

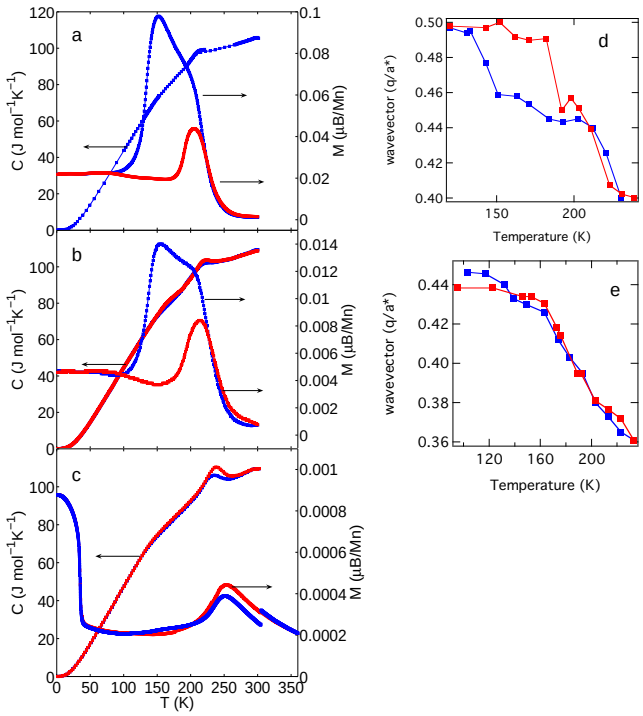

FIG. 1: Heat capacity, and magnetisation (in 100 Oe), with warming data shown in red and cooling data shown in blue. (a) shows data for $La_{0.50}Ca_{0.50}MnO_3$, (b) shows data for $La_{0.48}Ca_{0.52}MnO_3$, and (c) shows data for $Pr_{0.48}Ca_{0.52}MnO_3$. The errors are smaller than the size of the data points. The variation of the wavevector of the superstructure wavevector with T is shown for $La_{0.50}Ca_{0.50}MnO_3$ in (d) (data from [6]) and for $La_{0.48}Ca_{0.52}MnO_3$ in (e) (data from [12]).

than the system had reached equilibrium the heat capacity measurements were taken with very dense data points (between 140 and 600 measurements made between 1.8 K and 300 K), and the system was allowed around twenty minutes to reach equilibrium at each T (decreasing the waiting period to three minutes produced substantially different data in the regions of the transitions). The long relaxation times at each T hints at pinning of the superstructure to defects in the system [23]. Magnetic susceptibility measurements were performed using a Quantum Design Magnetic Properties Measurement System. Samples with masses between 30 and 45 mg were used.

The heat capacity data for all three compounds show two transitions (see Fig. 1), with the transition at higher T exhibiting a much larger change in entropy than the lower transition. In order to make the transitions more visible the background was removed from the data. In the low T (1.8 K - 10 K) range, heat capacity data were fitted to an equation of the form:

$$C_{\rm P} = \beta_3 T^3 + \beta_5 T^5 + \gamma T + \frac{\alpha}{T^2} + \delta T^2 \ , \qquad (1)$$

where β_3, β_5, α, δ and γ are constants, $\beta_3 = Nk\frac{12\pi^4}{5}\frac{1}{\theta_D^3}$, where θ_D is the Debye T [24]. The high T data is modelled with a Debye model and an Einstein mode, where $\theta_{\rm D}$ has been determined from the low T data. The data were fitted with iterative reweighted least squares [25] using the Levenberg-Marquardt method [26]. This method has the advantage over the more commonly used least-squares technique that low weights are automatically given to areas which have a poor fit to the model (so the errors are not assumed to be Gaussian). The heat capacity above background is shown in Fig. 2a,b, and c.

As can be seen from Figs. 1d, 1e, 2a and 2b the appearance of the superlattice reflections occurs at the same T as the upper transition, and the stabilisation of the value of the wavevector occurs at the same T as the lower transition. This indicates that the evolution of the superstructure is strongly linked to the phase transitions. The Ts of the transitions (see Table II) for both $La_{0.48}Ca_{0.52}MnO_3$ and $Pr_{0.48}Ca_{0.52}MnO_3$ show hysteresis. The lower transition shows greater T hysteresis than the upper transition, probably since at the lower T the superstructure has become more strongly pinned to grain boundaries and impurities in the lattice.

The magnetisation data for $La_{0.50}Ca_{0.50}MnO_3$ and $La_{0.48}Ca_{0.52}MnO_3$ show an increase in magnetic moment on cooling corresponding to a transition of some proportion of the sample to FM (see Fig. 1). At lower Ts the magnetisation falls again - this is traditionally associated with the transition to AFM [27]. In the T range between the two transitions hysteresis is observed in M-H loops (see Fig. 3).

The presence of an FM-AFM transition in $La_{0.50}Ca_{0.50}MnO_3$ and $La_{0.48}Ca_{0.52}MnO_3$ agrees with the suggestion of Milward *et al.* [14] that charge order which has not locked into its low T value will always be associated with ferromagnetism. The magnetisation is higher for $La_{0.50}Ca_{0.50}MnO_3$ than for $La_{0.48}Ca_{0.52}MnO_3$, as predicted by Landau theory [14].

The magnetisation for $Pr_{0.48}Ca_{0.52}MnO_3$ shows a small change in the region of the transitions. However, the magnitude of the magnetisation for $Pr_{0.48}Ca_{0.52}MnO_3$ is only 1% of that for $La_{0.50}Ca_{0.50}MnO_3$. However, there is also a marked increase in the magnetic moment below 50 K which is not associated with any obvious features in the heat capacity data. However, the $La_{0.48}Ca_{0.52}MnO_3$ and $Pr_{0.48}Ca_{0.52}MnO_3$ heat capacity data do show a constant difference (on average 8%) in the range 20 - 100 K (see Fig. 2), with an extra entropy of 5.1 J mol^{-1} K^{-1} arising in $Pr_{0.48}Ca_{0.52}MnO_3$ relative to $La_{0.48}Ca_{0.52}MnO_3$ in this T range. Since the masses of Pr and La differ by only 1.4%, the change in the phonon contribution to the heat capacity is unlikely to have produced the large observed difference [28]. Thus there may be a magnetic phase in $Pr_{0.48}Ca_{0.52}MnO_3$ which evolves continuously between 2 and 50 K.

The calculated entropies (see Table III) are lower by a factor of around two than those found in other studies of

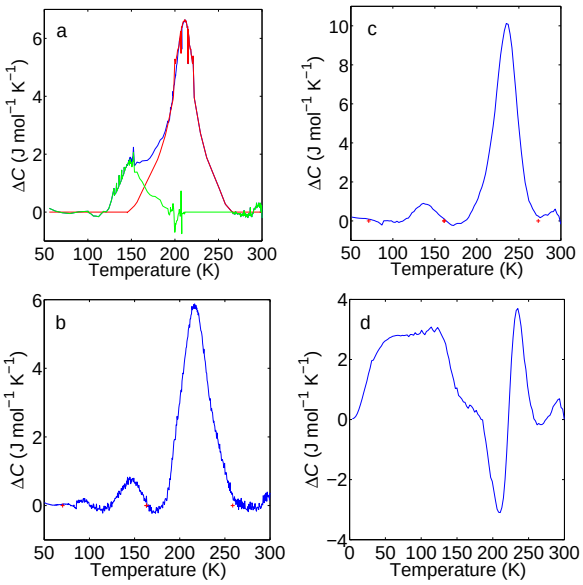

FIG. 2: Excess heat capacity of (a) $La_{0.50}Ca_{0.50}MnO_3$, (b) $La_{0.48}Ca_{0.52}MnO_3$ and (c) $Pr_{0.48}Ca_{0.52}MnO_3$ with background removed. (d) $La_{0.48}Ca_{0.52}MnO_3$ heat capacity subtracted from $Pr_{0.48}Ca_{0.52}MnO_3$ heat capacity. In (a) the blue line is total heat capacity above background. The red and green lines show the contributions of the upper and lower T transitions respectively. In (b) and (c) the red crosses signify the limits used for the entropy calculation.

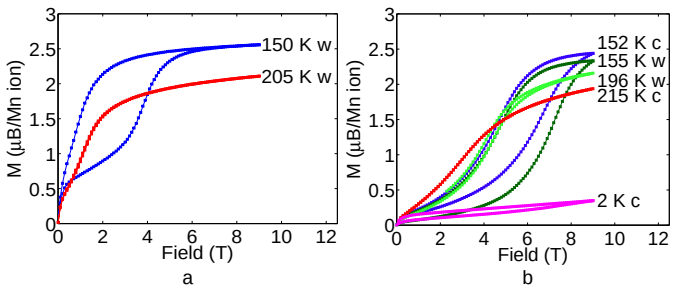

FIG. 3: M-H loops taken at various Ts on warming and cooling for (a) $La_{0.50}Ca_{0.50}MnO_3$ and (b) $La_{0.48}Ca_{0.52}MnO_3$. Curves were taken on warming (w) and cooling (c).

similar compounds [15, 29]. This difference is probably due to the fact that the entropies in Refs. [15, 29] were calculated by fitting a polynomial away from the region of the transitions, rather than using all of the data to fit a background which is smooth in the region of the transitions, as done in the present work.

We now show that the two transitions are dominated by electron-lattice effects associated with the superstructure. At the upper transition, the percentages of the total entropy are the same in $La_{0.50}Ca_{0.50}MnO_3$ and $La_{0.48}Ca_{0.52}MnO_3$ (the absolute values are only 28% different), despite the fact that the magnetisation is ten times smaller in $La_{0.48}Ca_{0.52}MnO_3$. In $Pr_{0.48}Ca_{0.52}MnO_3$ the entropy of the upper transition is higher than that in $La_{0.50}Ca_{0.50}MnO_3$ and $La_{0.48}Ca_{0.52}MnO_3$, despite the fact that the magnetisation is 100 times smaller in $Pr_{0.48}Ca_{0.52}MnO_3$ than in $La_{0.50}Ca_{0.50}MnO_3$. Since $Pr_{0.48}Ca_{0.52}MnO_3$ is expected to have stronger electron-phonon coupling than $La_{0.48}Ca_{0.52}MnO_3$, this indicates that the electron-phonon coupling is dominating the value of the released entropy. Thus the entropy of the upper transition is dominated by electron-lattice effects, and shows little or no link with the magnetisation. The proportion of entropy released at the lower transition for $Pr_{0.48}Ca_{0.52}MnO_3$ is only lower than the values for $La_{0.50}Ca_{0.50}MnO_3$ and $La_{0.48}Ca_{0.52}MnO_3$ by a factor of two, although the magnetic transition has all but disappeared. Thus even the lower transition is not dominated by magnetic effects.

When passing through a first order transition, the sample should emit latent heat, producing a PPMS decay curve that cannot be well modelled by the analysis software [22]. Therefore, decay curves were examined in the regions of the transitions, but the values derived manually were the same as the values which had been determined automatically, within experimental error. This absence of latent heat at the transition is the first piece of evidence that the transitions are second order.

The second piece of evidence that the upper transition is second order is that the heat capacity peak is always asymmetric (see figure 2). A second order transition in a very pure sample can be modelled using critical exponents; however, the breadth of the peak in this case indicated that a model including impurities must be used. Therefore the heat capacity peak above background at the transition was modelled as a Peierls transition in a system containing impurities [30]:

$$C \propto \frac{d\chi}{dt} \propto \frac{d\kappa_{\rm imp}}{dt} \propto \frac{d}{dt}\{(-t) + [(-t)^2 + N^4]^{1/2}\}^{1/2} \quad (2)$$

where χ is the magnetic susceptibility, $\kappa_{\rm imp}$ is the inverse ionic correlation length in the presence of impurities, $N = \Lambda x^{1/d}$ and $t = (T - T^*)/T^*$. Λ is an input lengthscale determined by the impurity potential (taken to be roughly a lattice spacing), d is the system dimension, x is the impurity concentration and $T^* = T_{\rm C}^{\rm imp} = T_{\rm C}^{\rm pure} - \Delta T$. Since the low and high T limits of this function are not the same, a linear background was subtracted to enable the function to be fitted to the heat capacity above background. The fit can be made over the widest range for $Pr_{0.48}Ca_{0.52}MnO_3$ because the upper transition is well separated from the lower transition. For $La_{0.50}Ca_{0.50}MnO_3$ and $La_{0.48}Ca_{0.52}MnO_3$ the lower transition is close, and therefore the fit must be made over a narrower range. As can be seen from Fig. 4, the model provides an extremely good fit to the data.

A lengthscale for the disorder was calculated as $x^{-1/d} = \Lambda/N$. For $Pr_{0.48}Ca_{0.52}MnO_3$ and $La_{0.50}Ca_{0.50}MnO_3$ the result was 23 Å, and for

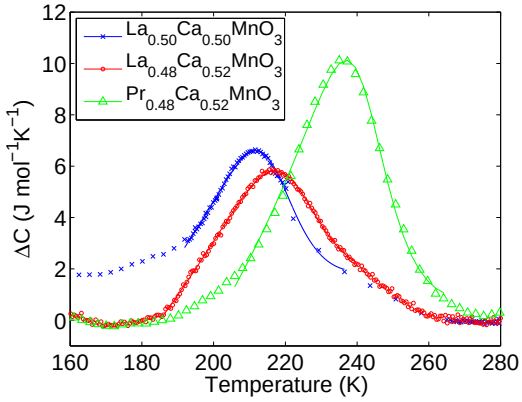

FIG. 4: Fitting of transition peaks for $La_{0.50}Ca_{0.50}MnO_3$, $La_{0.48}Ca_{0.52}MnO_3$ and $Pr_{0.48}Ca_{0.52}MnO_3$ to a model of a Peierls transition in a system with impurities (a linear background was removed). Points are data and the solid line is the fit of the model to the data.

	Lower transition (K)		Upper transition (K)	
	cool	warm	cool	warm
$La_{0.50}Ca_{0.50}MnO_3$	150	-	223	-
$La_{0.48}Ca_{0.52}MnO_3$	146	158	218	223
$Pr_{0.48}Ca_{0.52}MnO_3$	131	138	229	234

TABLE II: Transition Ts for $La_{0.50}Ca_{0.50}MnO_3$, $La_{0.48}Ca_{0.52}MnO_3$ and $Pr_{0.48}Ca_{0.52}MnO_3$.

$La_{0.48}Ca_{0.52}MnO_3$ it was 21 Å. Therefore the lengthscale of the disorder is very similar in all three compounds. By comparison, blue bronze (a charge density wave system) doped with 1% W ($K_{0.3}Mo_{0.99}W_{0.01}O_3$) yields a lengthscale of 51Å. The fact that this model can fit all three compounds, with similar disorder lengthscales, supports the conjecture that the transition is a Peierls transition in disordered materials. We suggest that the 'impurities' may in fact reflect the A-site cation inhomogeneity rather than chemical inhomogeneities since x-ray and neutron data indicate that the samples are single phase [13, 21].

In conclusion, our data showed that the upper transition which has been traditionally associated with the onset of FM in $x = 0.5$ is in fact driven by the lattice.

	S of lower transition		S of upper transition	
	J/(mol K)	% of S_{tot}	J/(mol K)	% of S_{tot}
$La_{0.50}Ca_{0.50}MnO_3$	0.41	24	1.33	76
$La_{0.48}Ca_{0.52}MnO_3$	0.25	21	0.95	79
$Pr_{0.48}Ca_{0.52}MnO_3$	0.21	13	1.36	87
$Pr_{0.6}Ca_{0.4}MnO_3$	0.6	23	2.0	77
$La_{0.25}Ca_{0.75}MnO_3$	0.67	23	2.3	77

TABLE III: Entropy values for the transitions in various manganite compounds. Data for $Pr_{0.6}Ca_{0.4}MnO_3$ taken from [15], data for $La_{0.25}Ca_{0.75}MnO_3$ taken from [29].

The transition is second order, and can be well modelled as a Peierls transition in a disordered material. The previous conclusion that the transition was first order was based merely on hysteresis in the resistivity data [17], rather than on the measurement of any thermodynamic quantity. Such hysteresis can be explained as being due to lossy kinetics in a CDW-like ground state with disorder [13]. Other work assumes this transition is first order [18] since the electron-phonon coupling is taken to be large. As we have shown, the electron-lattice effects are dominant, but can be well modelled as a CDW in which insulating behaviour can be produced without the need to invoke strong electron-phonon coupling. Finally, an unexpected low T magnetic phase has been found in $Pr_{0.48}Ca_{0.52}MnO_3$ which evolves continuously at low T.

We thank N.D. Mathur and N. Harrison for helpful comments. Work at NHMFL is performed under the auspices of the NSF, DoE and the State of Florida. Work at Cambridge was funded by the UK EPSRC and the Royal Society. S. Cox acknowledges support from the Seaborg Institute.

[1] S. Mori *et al.*, Nature **392**, 473 (1998).
[2] C.H. Chen *et al.*, J. Appl Phys **81**, 4326 (1997).
[3] J.M. Tranquada *et al.*, Nature **375**, 561 (1995).
[4] C.H. Chen *et al.*, Phys. Rev. Lett. **71**, 2461 (1993).
[5] T. Vogt *et al.*, Phys. Rev. Lett. **84**, 2969 (2000).
[6] C.H. Chen, S.-W. Cheong, Phys. Rev. Lett. **76**, 4042 (1996).
[7] J. Rodriguez-Carvajal *et al.*, Physica B **320**, 1 (2002).
[8] A. Daoud-Aladine *et al*, Phys. Rev. Lett. **89**, 097205 (2002).
[9] E.E. Rodriguez *et al.*, Phys. Rev. B **71**, 104430 (2005).
[10] R.J. Goff, J.P. Attfield, Phys. Rev. B **70**, 140404(R) (2004).
[11] G. Subias *et al.*, Phys. Rev. B **56**, 8183 (1997).
[12] J. C. Loudon *et al.*, Phys. Rev. Lett. **94**, 097202 (2005).
[13] S. Cox *et al.*, *preprint* (2006).
[14] G.C. Milward *et al.*, Nature **433**, 607 (2005).
[15] M.R. Lees *et al.*, Phys. Rev. B **59**, 1298 (1999).
[16] A.P. Ramirez *et al.*, Phys. Rev. Lett. **76**, 3188 (1996).
[17] M. T. Fernandez-Diaz *et al.*, Phys. Rev. B **59**, 1277 (1999).
[18] A.P. Ramirez, S.-W. Cheong, P. Schiffer, J. Appl. Phys. **81**, 5337 (1997).
[19] J. C. Loudon *et al.*, Phil. Mag. **85**, 999 (2005).
[20] R.D. Shannon, Acta. Cryst. A **32**, 751 (1976).
[21] A.J. Williams *et al.*, J. Sol. State Chem. **173**, 456 (2003).
[22] J.C. Lashley *et al.*, Cryogenics **43**, 369 (2003).
[23] G. Grüner, *Density waves in solids* (Addison-Wesley, 1994).
[24] P. Debye, Annalen der Physik **39**, 789 (1912).
[25] P. J. Huber, *Robust Statistics* (Wiley, 1981).
[26] D. Marquardt, SIAM J. Appl. Math. **11**, 431 (1963).
[27] S.-W. Cheong, H.Y. Hwang, in *Colossal magnetoresistive oxides*, edited by Y. Tokura (Gordon and Breach, 2000), pp. 237–280.

[28] J. Loram, *Private communication* (2005).
[29] R.K. Zheng *et al.*, J. Appl. Phys. **94**, 514 (2003).
[30] P. Chandra, J. Phys. Condens. Matter **1**, 10067 (1989).